Int. Agrophys., 2011, 25, 37-46

INTERNATIONAL
Agrophysics
www.international-agrophysics.org

Use of DEM and ASTER sensor data for soil and agricultural characterizing

H.R. Matinfar[1]*, *F. Sarmadian*[2], *and S.K. Alavipanah*[3]

[1]Department of Soil Science Engineering, University of Lorestan, Khormabad, Iran
[2]Department of Soil Science Engineering, University of Tehran, Tehran, Iran
[3]Department of Cartography, University of Tehran, Tehran, Iran

Received March 15, 2010; accepted October 20, 2010

A b s t r a c t. The objective of this study was to evaluate the role of ASTER and digital elevation model (DEM) data for classifying soils and agricultural lands. The obtained results from the image processing and spectral reflection revealed that the green plants have higher reflection in near infrared than wilted and bare soils. The results also demonstrated that that the highest reflections in visible and middle infrared are mainly related to the saline and gypsiferous soils. Besides, the lowest reflection of the saline soils is attributed to for the semi-wet soils with bright salt crusts. It is due to the moisture effect and sponge like surfaces of the crusts that can be due to a great absorbtion in sun radiations. All ASTER bands are able to separate the stony, rough and uneven land classes from the homogenous saline soils wit the soft and black appearance. Based on the obtained results we may generally conclude that for separating the saline classes with different surface characteristics digital elevation model (DEM) has a key role in improving accuracy. This result also indicated that the visible and near infrared bands can be mainly used for separating the salt crust soils from some other soil classes.

K e y w o r d s: ASTER, DEM, bare soil, arid zones, supervised classification

INTRODUCTION

Soil is an essential part of terrestrial ecosystem. Many soil scientists, technicians, and farmers have studied its physico-chemical properties for many years for agriculture and soil conservation. This should usually require field sampling and laboratory analysis that are time-consuming and destructive to the samples being analyzed. Remotely sensed data are an alternative that provide reliable information at low cost based on a non-destructive technique (Chuvieco and Huete, 2010). The use of remote sensing imagery for mapping, assessing and monitoring of agricultural crop conditions and production has been steadily increasing in recent years. Air-borne and/or space borne imaging systems are now increasingly being used for various spatial-temporal scales at different mapping objectives and implementation levels.

One of the methods of soil and other land cover type characteristics recognition is the remote sensing and study of spectral reflectance of the surface cover types (Piekarczyk, 2001; Yuan *et al.,* 2005). Soil is a complex phenomenon, and the spectral reflection of that, is the resultant of soil physicochemical characteristics. Thus, using physical models in order to study the spectral attributes of soil is difficult (Clark and Roush, 1984; Law *et al*., 2003; Shalaby and Tateishi, 2007). Using ancillary information such as advanced very high resolution radiometer (AVHRR) data and digital elevation model (DEM) derivatives from the national to continental level surveys is among the most promising tools for geographers and soil surveyors (Ali and Kotb, 2010; Dobos *et al*., 2000). DEM is increasingly incorporated in agriculture, natural resource management, engineering, geographical information system (GIS) and remote sensing analysis, partly because of the wide range of potential applications, and partly because of trend from two dimensional to three dimensional spatial data capture and visualization (Shrestha and Zinck, 2001, Aboudel-magd and Tantont, 2003). The integration of image processing and spatial analysis functions in GIS improved the overall classification accuracy result from 67 to 94%. Fahsi *et al*. (2000), showed that DEM data considerably improved the classifcation accuracy by reducing the effect of relief on satellite images. The variation coefficient for homogeneous cover type areas was substantially reduced for all the spectral bands on the corrected image. Consequently, the overall accuracy and the

*Corresponding author's e-mail: matinfar44@gmail.com

Kappa coefficient were notably improved on the corrected image. The individual accuracies of the different classes also increased.

Buhe *et al*. (2007) used ASTER (Advanced Spaceborne Thermal Emission and Reflection Radiometer) data for recognition of land covers at a region in China. 3 band combinations for coloured image are very difficult because the 14 bands would have 364, three combinations. Thus, an index was tried instead of the 3 band combination. The index was based on the total variance and the least correlation coefficient of the bands. The suggested index was to be highly useful. Satio *et al*. (2001), prepared farm land soils using ASTER data analysis comparison of the map with current map is evidence for the good conformity of them. Interaction between cover attributes *eg* same wheat but in an early stage or in a very wet patch produced some classification errors. Breunig *et al*. (2009), used ASTER sensor data in order to soil studies, results showed emissivity and elevation data revealed variations in soil composition with topography in specific parts of the landscape. Despite that, ASTER sensitivity to changes in biophysical conditions indicates that these data are useful for mapping within-field variability where the focus is confined to a limited area. The three bands that produced the best average separability are the layers pertaining to vegetation indices: ratio NIR (Near Infra REd) /R (Red), Sqrt (NIR/R) and NIR-R. The aim of this study is to analyze the seperability of arid zone soils using the 14 ASTER bands. It is often regarded that the spectral data, of the local biophysical setting and crop calendar information, is useful in a broad-level crop type discrimination and plant stress detection (Cloutis, 1999). Recently launched satellite based imaging sensors, equipped with improved spatial, spectral and radiometric resolutions, offer enhanced the capabilities in comparison of the previous systems.

The aim of this study is investigate the utility of ASTER multispectral data, that is integrated with digital elevation model, as an ancillary and improved method for characterizing agricultural and bare land. Evaluation of visible short wave infrared and thermal infrared, data of the sensor, for recognition of arid saline and non saline soils and also soils with various amounts of stoniness and crusts is possible to be separated by this method.

MATERIALS AND METHODS

The study area is located in Esfahan province (34°-34° 30‘N, 50°- 50° 15‘E). It is the partially area of central kavir of Iran (Fig. 1). Aran region has long-term and warm summers and temperate winters. Average annual rainfall was 138.8 mm (30 years). The precipitation starts from November and ends in April. Temperature and moisture regime of the soils of this area is thermic and aridic, respectively.

In order to asses satellite data capability in separation of lands from ASTER sensor data, topographic map, geo- logy map and field study were used. The study was carried out in six stages:

1 - initial image processing,
2 - field study,
3 - separation of photomorphic units on images (PMU),
4 - digital elevation model (DEM) generation,
5 - images classification and accuracy assessments,
6 - post classification.

An attempt was made to evaluate the lands separability, mean standard deviation and for the variance of test samples. ASTER is the second sensor in the set of EOS astronomy. This has been put on TERRA Platform in 1991 by America and Japan. ASTER consists of three different subsystems:

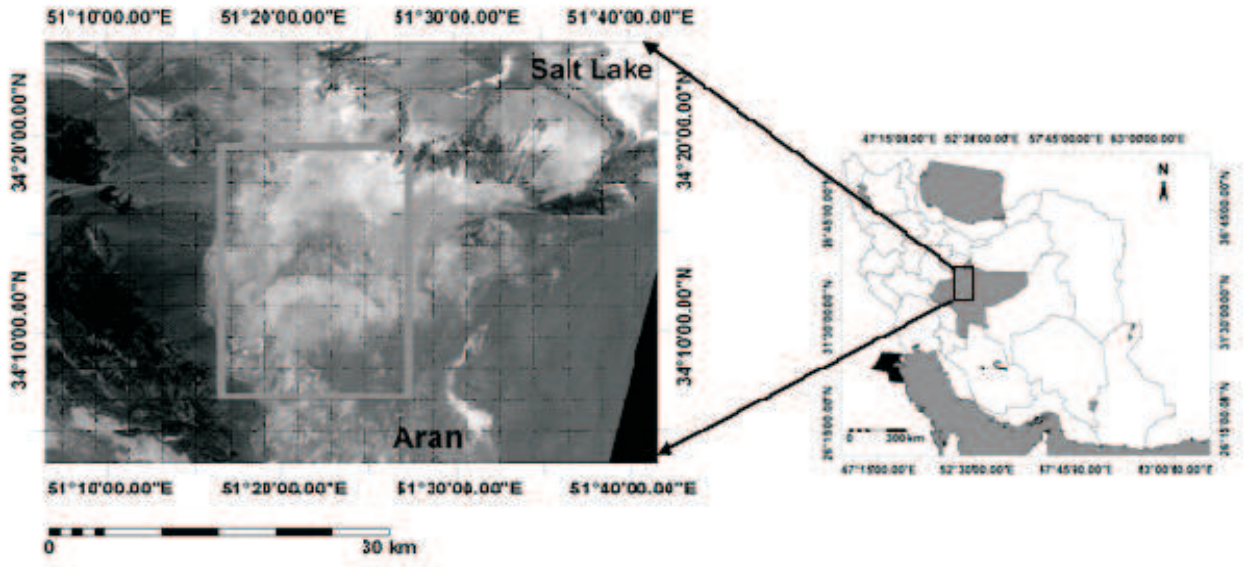

Fig. 1. Location of the study area in Esfahan province, Iran.

– the visible and near-infrared (VNIR) has three bands with a spatial resolution of 15 m, and an additional backward telescope for stereo;
– the shortwave infrared (SWIR) has 6 bands with a spatial resolution of 30 m;
– the thermal infrared (TIR) has 5 bands with a spatial resolution of 90 m.

Each subsystem operates in a different spectral region, with its own telescopes, and is built by a different Japanese company. The spectral band passes are shown in Table 1. In addition, one more telescope is used to view backward in the near-infrared spectral band (band 3B) for stereoscopic capability. In this study, ASTER-L1B Images which are relevant to the date August 10, 2002 was used. The received data are having Geotiff format which were read by ILWIS 3.3.The images were registered to topographic maps of 1:50000 scale which have 16 control points and the UTM as a projection system were accepted.

Height values were added as attributes to the contour vectors derived from the 20 m contour separations. Height values of the contour lines were interpolated to create raster-based DEM (Figs 2 and 3), using GIS software as:

T a b l e 1. Different combination of digital layers

Composition No.	ASTER bands														Transformed layer	
	1	2	3	4	5	6	7	8	9	10	11	12	13	14	DEM	BI, PC1, PC2, PC3, PC4
1	*	*	*	*	*	*	*	*	*	*	*	*	*	*		
2	*	*	*	*	*	*	*	*	*	*	*	*	*	*	*	
3	*	*	*						*							
4	*	*	*						*						*	
5	*		*							*	*					
6	*		*							*	*				*	
7																*
8	*	*	*	*	*	*	*	*	*		*					
9	*	*	*	*	*	*	*	*	*		*				*	
10	*	*	*	*	*	*	*	*	*				*			
11	*	*	*	*	*	*	*	*	*				*		*	

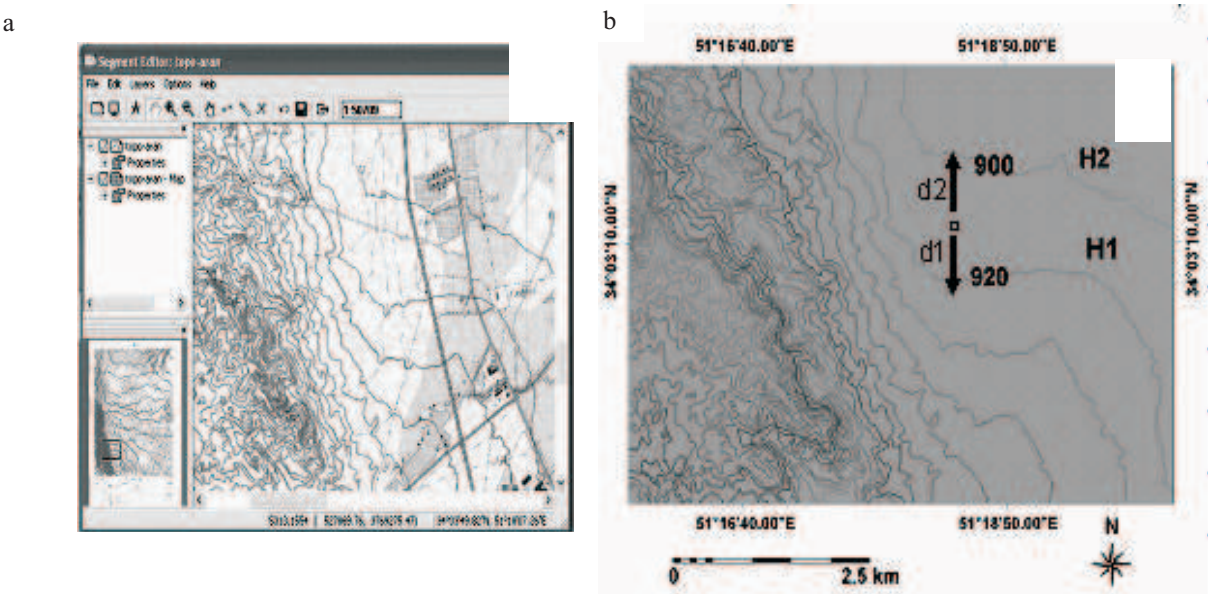

Fig. 2. On screen digitizing of counter line (a) and vector to raster transformation and interpolation to DEM generation (b).

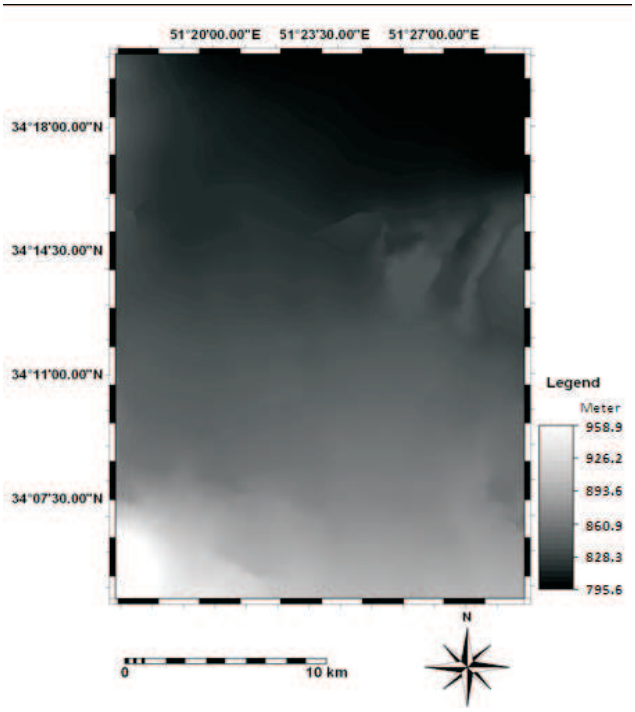

Fig. 3. Digital elevation model of study area.

$$Hp = H_1 + (D_2/(D_1+D_2))(H_1-H_2) \quad (1)$$

where: H_p – value of output pixel, H_1, H_2 are value of contour line, D_1, D_2 are output pixel distance to contour line.

The accuracy of DEM was also investigated by comparing the elevation figures of ten locations with the original topographic map. Figure 4 shows the diagram of ASTER data integrated with DEM in order to soil and agricultural land characterizing.

Selection of suitable bands is one of the major levels prior to digital data processing and getting the spectral information. The three – composites resulted from 14 spectral bands equals 364 combinations. Study and selection of a suitable combination out of them is time consuming and expensive with lots of errors. Thus, uses of statistical indices are profitable in terms of expressed, true accuracy in bands selection and saving the time. Therefore optimum index factors are calculated once for the 14 bands of the sensor and one more time for the thermal bands. Results of principal component analysis of ASTER data indicate that around 99% of the information is concentrated in the PC1 toPC4.

Also, the false colour composite image of PC1, PC2 and PC3 are well displayed saline and gypsic lands, lands having more than 35% stoniness and lands having soft crusts. The image resulted of brightness index is displayed of saline

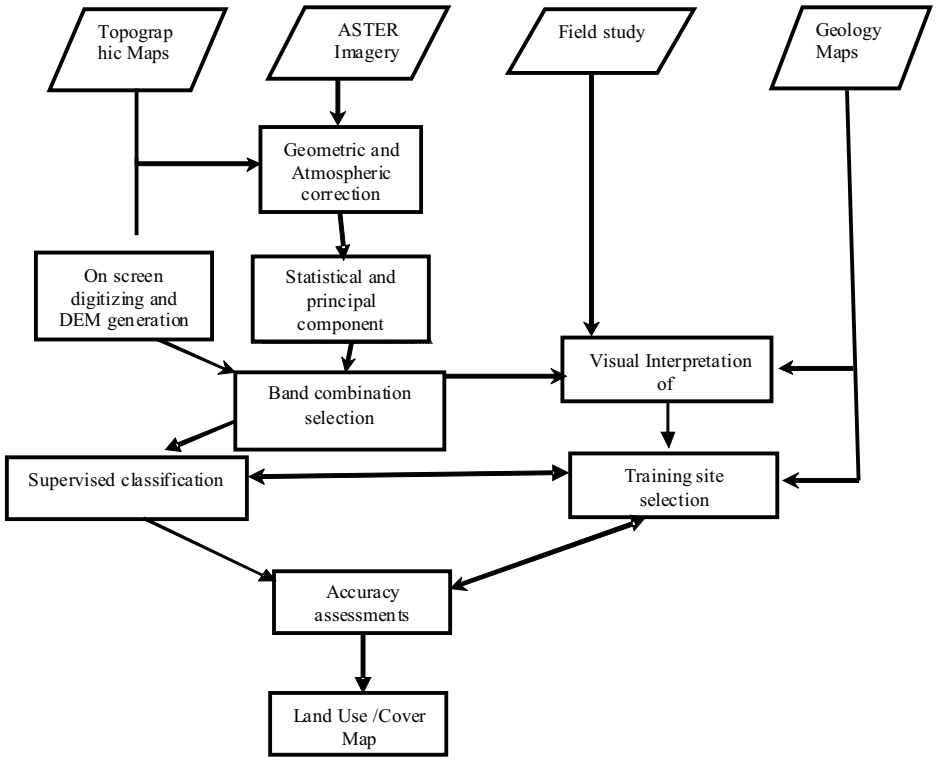

Fig. 4. Diagram of agricultural land and soil characterizing based on ASTER data and DEM.

lands with more clearance. In order to assess the importance of 14 bands, different band combination have been prepared. The combinations, consisting of the sensor bands, indices and combinations of optimum index factor (Table 1).

Table 2 is the bands correlation which show 11, 12, 13 and 14th bands (8. 125-11.65 μm) having inverse correlation with visible (VNIR) and shortwave infrared (SWIR) bands. The 13 and 14th bands having high correlation with one another and the trend of their correlation with other bands stay constant. The 1and 2 bands of the visible range have high correlation to each other but less correlation with middle infrareds. The correlation trend of the VNIR and SWIR bands are almost the same but the cause of their difference, is the correlation degree of them. Thus, low correlation of the thermal bands with VNIR and SWIR, implies good information in the bands.

According to visual interpretation of photomorphic units on false colour composite images (FCC_{321}), 18 training classes (Table 3) were recognized and along with feature space displaying, the training zone pixels were chosen. In order to choose samples which are homogenous and of enough distribution on the image, all the images were analyzed as smaller windows, on choosing the samples, feature space of them were drawn and assessed to segment the classes. In the end the samples were corrected by using mean, standard deviation, feature space and spectral curve of them.

In each information – spectral class and subclass (Table 3) which have homogenous reflection on images, some parts of them were chosen as training samples Coordinates of the above mentioned regions were taken out and saved as point file in ILWIS, and then the file was saved in GPS. The sites distribution in the units is based on stratified random sampling, that is, around 4 to 8 sites were selected in each photomorphic unit on a scale of which surface. In order to increase the sampling accuracy, each site was selected in a region where is introducer to a significant area and the region does have the least disturbance and maximum homogeneity in terms of ground truths. Sites of saline and barren lands were selected in a way that each site has area of 10 ha at least, and bare surface or a surface having the least vegetation cover. Agricultural sites, formed forests and tree groups, were selected in order to be recognized. Acceptable method for evaluating image and the corresponding ground pixels is the sampling of 4×4 pixel area (Ben-Dor, 2001; Matinfar, 2006).

Thus, in each 4×4 pixel (where GPS located) the samples were taken from the control and the 4 pixels around the central pixel. The sites are including the profile, auger and surface sampling points. Then surface samples of each site were mixed together (composite sample) and around 2 kg of which were taken to soil laboratory for physicochemical analysis, all the visible ground truth and outcrops of each site were recorded that is, a quantitative and descriptive sheet of the sites was written in which coordination system of the sites was taken down in UTM.

RESULTS AND DISCUSSION

As explained earlier, upon separation of homogenous units (PMU) homogenous areas for each class are chosen on the monitor. Note that the training samples are selected according to their distribution of them in the spectral space

T a b l e 2. Correlation matrix between ASTER data in Aran area

	B1	B2	B3	B4	B5	B6	B7	B8	B9	B10	B11	B12	B13	B14
B1	1													
B2	0.98	1												
B3	0.76	0.77	1											
B4	0.85	0.9	0.85	1										
B5	0.81	0.86	0.67	0.92	1									
B6	0.79	0.84	0.66	0.9	0.99	1								
B7	0.8	0.86	0.66	0.9	0.99	0.99	1							
B8	0.82	0.87	0.66	0.9	0.98	0.99	0.99	1						
B9	0.68	0.75	0.54	0.8	0.95	0.97	0.96	0.96	1					
B10	-0.16	-0.08	-0.42	-0.1	0.04	0.04	0.03	0.02	0.09	1				
B11	-0.24	-0.17	-0.51	-0.18	0	0.01	0	-0.01	0.1	0.96	1			
B12	-0.11	-0.05	-0.42	-0.08	0.07	0.07	0.07	0.06	0.12	0.97	0.97	1		
B13	-0.07	0	-0.37	-0.03	0.13	0.12	0.13	0.11	0.17	0.98	0.94	0.97	1	1
B14	-0.07	0	-0.37	-0.03	0.12	0.11	0.12	0.11	0.16	0.98	0.94	0.96	1	1

T a b l e 3. Information classes in Aran area

Information classes	Code	Soil name (U.S.D.A.)	Salinity class	Surface condition
Afforestation	AF	Typic Haplosalids	S4	Smooth crust, 20 to 60% canopy intensity
Bad Land	BL	–	–	Rill erosion, <5% canopy
Crop 1	FA1	Typic Haplocalcids	S1	Residual, bare soil
Crop 2	FA2	Typic Haplocalcids	S1	Crust, destroyed farm
Crop 3	FA3	Typic Haplocalcids	S0	Irrigated farm, intensity canopy
Crop 5	FA5	Typic Torrifluvents	S1	Residual
Crop 6	FA6	Typic Haplocalcids	S2	Cotton
Orchard	OR	Typic Torrifluvents	S0	*Prunus armenica, prunus domestica,punica granatum*, >60% canopy
Pasture	R3	Typic Haplosalids	S4	*Artemisia*, crust, 30 to 35% canopy
Sand Dune	SD	–	–	Sand accumulation, <5% canopy
Soil 2	S2	Typic Haplogypsids	S1	Gravel 30 to 35%, 30% gypsum
Soil 3	S3	Typic Torriorthents	S0	60 to 70% gravel, non saline
Soil 4	S 4	Typic Haplosalids	S4	Shrieked crust, very saline, bare soil
Soil 5	S5	Typic Haplosalids	S4	Smooth and puffy crust, very saline, bare soil
Soil 6	S6	Gypsic Aquisalids	S4	Gypsum and salt, very saline, bare soil
Soil 7	S7	Typic Aquisalids	S4	Salty crust, very saline, bare soil
Soil 9	S 9	Typic Aquisalids	S4	Very saline, bare soil, salty polygon

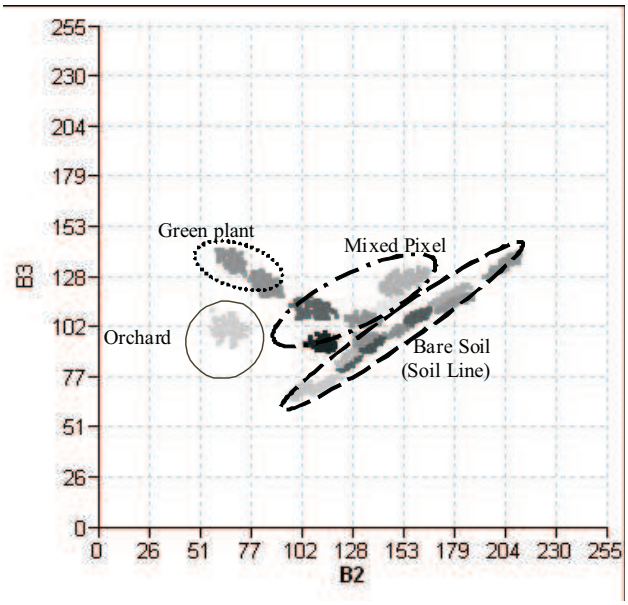

Fig. 5. Feature space B2 versus B3, show spectral-information class distribution.

of the selected bands. These samples must also have the same spectral characteristics. In order to know the pattern of the spectral classes, feature space of red band versus near infrared band was plotted. Feature space showed, Soil plant mixtures, plant residues, near harvest framings and green plants, distribution pattern (Fig. 5), in the lack of plant cover, soil line clusters are present, but as the plant intensity increases, the near infrared reflection increase and on the contrary red reflections reduces. Within the red band, chlorophyll is the cause of energy absorption and reflection reductions, but within the middle infrared the water in plants tissues absorbs the energy and reduces the reflections. Thus as the plant intensity increases the above mention ratios decreases, that is, in the triangle head and close to the zero point, the clusters are related to green plants and the base of the triangle is related to the bare soil.

Different band combination was classified. Total ASTER bands and DEM layer have a greatest accuracy, so feature space of this combination in order to asses the land cover class separation. The training samples are consisting of four groups (Fig. 5) that show a triangle which base (soil line) states kinds of soils, head states green cover and between states both soil and plant together. The first group is the bare

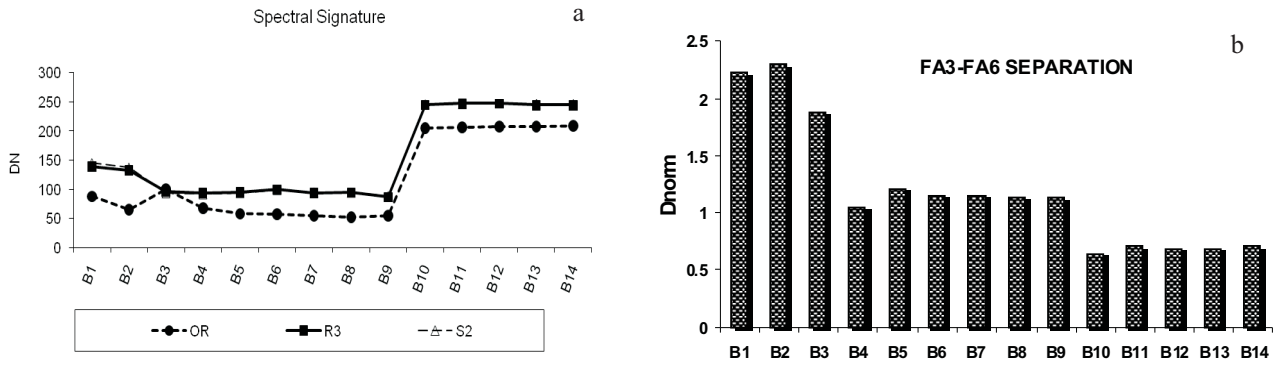

Fig. 6. Spectral curve of soil, pasture and green plant (a), separation between different canopies (b).

soil samples. It is distributed in the 2-dimensional space over the soil line, dark non saline soils, soil (3) and then saline and moist soils, soil (9) are distributed near the zero point. At the end of the line, saline and gypsic Soils, soil (5), soil (6) and soil (7) are distributed. The second group is the samples relevant to the mixture of soil and plant; on the other hand the farming (1), farming (2), pasture, farming (5) and afforestated classes. The third group is the samples relevant to orchards and the forth group is the green and healthy covers consisting of farming (3) and farming (6).

Green plants and tree groups , farming (6) , farming (3) and orchards have wore absorption of spectral range of red, because chlorophyll receives the energy and decreases the reflection amount (Fig. 6a). Note that the visible and reflective infrared bands are different in green plants cover separation, Fig. 6b shows ability of thermal bands in separation of green plants it seems that roughly similar moisture conditions of the green plants cover cause the least separation (lowest D_{norm}) in spectral range of thermal bands and mixed pixels formation.

$$D_{norm}=|\mu_1-\mu_2|/ (\sigma_1+\sigma_2) , \quad (2)$$

μ – class mean, σ – class variance.

Spectral curve of the bare soils states that salt and gypsum crystals presences with no moisture, cause increase in reflections and dark gravels as well as sponge like salt crusts with moisture, case reduction in the reflections. The Fig. 7a shows reflection of soil (3), soil (5), soil (6), soil (7) and soil (9). As it is seen, soil class (3) has the least reflection among all other bands and the soil class (6) has the most reflection. Soil class (3) indicates bare lands which have 60-70% dark brownish gravels without salinity and alkalinity signs, but the soil class (6) indicates non-gravelly saline and gypsic lands. Another look in the training areas graphs, expresses that, soil class (6) has the most reflection in all wave lengths, and white crystals of gypsum and salt on these soils surfaces cause the most reflection. In the lands while the soil class (9) which consists of saline and moist saline soil (lower layers), has the least reflection among saline classes. This is because the sponge – like crusts and moisture absorb the received energy and reduces refection.

Soil classes of 5 with 6 and 7 with 6 have confusion (Fig. 7a). Figure 7b shows that soils 6 and 7 have high ability in separation only in the range of visible and reflective infrared and the least ability in the range of other bands. Figure 7c shows soils 5 and 6 have high most separation only in the range of visible spectral. It seems that the spectral behaviours of salt and salt crusts within shortwave and theme infrared is important factor of mixed pixel formation.

According to the results of different step of classification the second combination has the highest and the seventh combination the least overall, user and producer accuracy and kappa coefficient (Table 4). The 3rd and 5th have the most amount of optimum index factor (OIF), But the accuracy is less than other band combination, which seems the interference cases in classification accuracy increase than optimum index for arid regions. As the table 4 gives, the Kappa coefficient is less than overall accuracy the reason is the reduction of chance in the coefficient calculation because other elements as well as diagonal elements of the error matrix are considered in the calculation.

One of the important factors that affect the accuracy of classified results is different feature with similar reflectance such as soil (3) and soil (9). But combination of effective layer such as DEM with ASTER bands make it possible to separate each feature, so increase the accuracy of these land cover (Fig. 8). Also Tajgardan *et al*. (2010),showed similar results in their study of prediction the spatial variability of surface soil salinity in an arid area in northern Iran.

Table 4 show the classifications accuracy, for the second combination the overall accuracy is 79, 66%, kappa coefficient 0.781 and producer and user accuracy are 85.86 and 86.86%, respectively (Jensen, 1996; Lillesand, 2004). How much the kappa is more, representing better classification. If

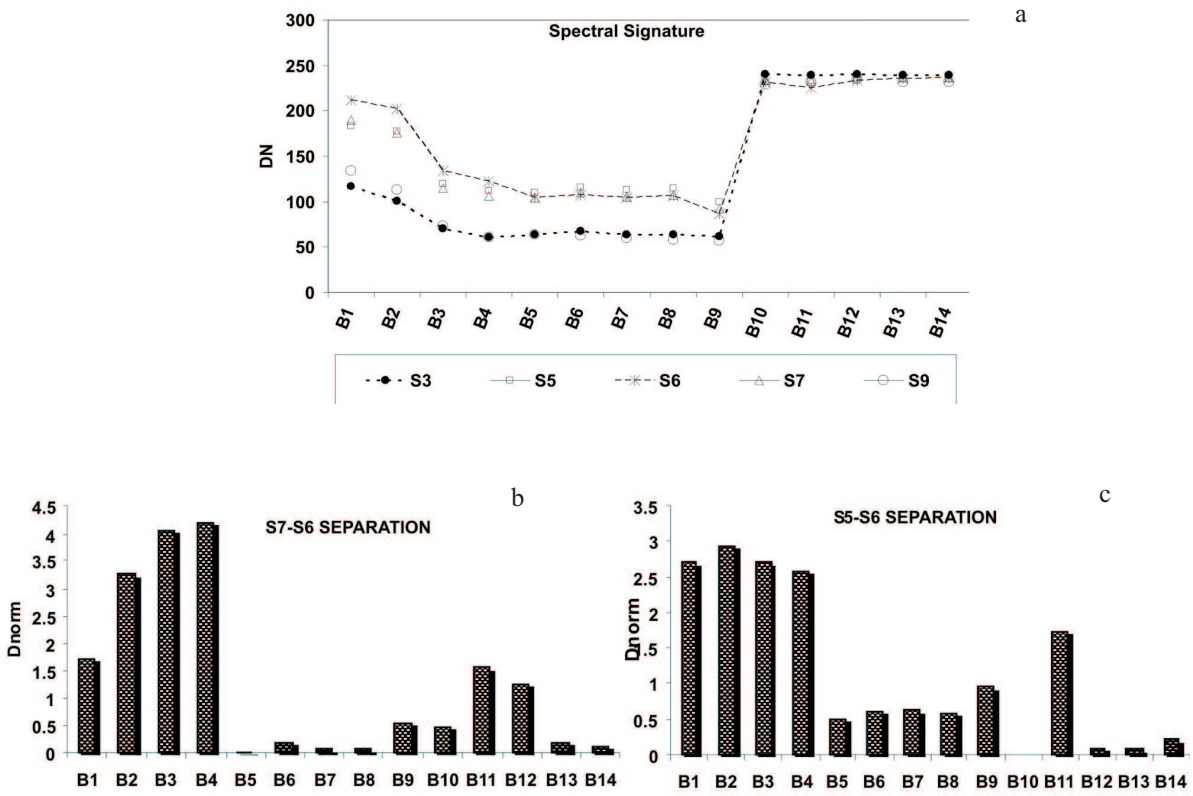

Fig. 7. Spectral reflectance of saline and non saline soils (a), separability of saline soils (b) and (c).

T a b l e 4. Accuracy assessment results

Combination	Producer accuracy	User accuracy	Overall accuracy	Kappa coefficient
Total ASTER bands	80.1	79.2	74.4	72.5
Total ASTER bands and DEM	85.9	86.9	79.7	78.1
1, 2, 3rd ASTER bands	73.4	73.5	65.8	61.5
1, 2, 3rd ASTER bands and DEM	80.3	81.2	74.1	71.5
1, 3, 10 and 11th bands	73.5	72.8	65.8	63.5
1, 3, 10 and 11th band and DEM	80.1	80.8	73.3	71.3
BI, PC1, PC2, PC3, PC4	56.5	52.2	48.0	45.5

all of the classes are classified correctly the kappa will be 1. As the non-diagonal pixels amount decreases the kappa will increase which is sign of error reduction in the classification. Among the bare lands classes, soil (3) has the highest producer and user accuracy which are 92 and 100%, respectively. The classes are of different conditions from others, for having 60-70% dark gravels on surface and 95% in profile, and also, having the highest elevation in the study area. Thus, on overlaying the spatial information of the classes, the classes are separated with more accuracy than others.

CONCLUSIONS

1. ASTER sensor spectral bands does separate healthy green plant covers from scattered covers and soil plant mixture, but lands of soil and plant mixture, have interference with non saline and gravely land. It also shows that soils having salt crust (soil 7) which are covered by salt, gypsum and sand (soil 6) are separated by visible and near infrared bands, but not in the thermal range for the similar behaviour of energy radiation.

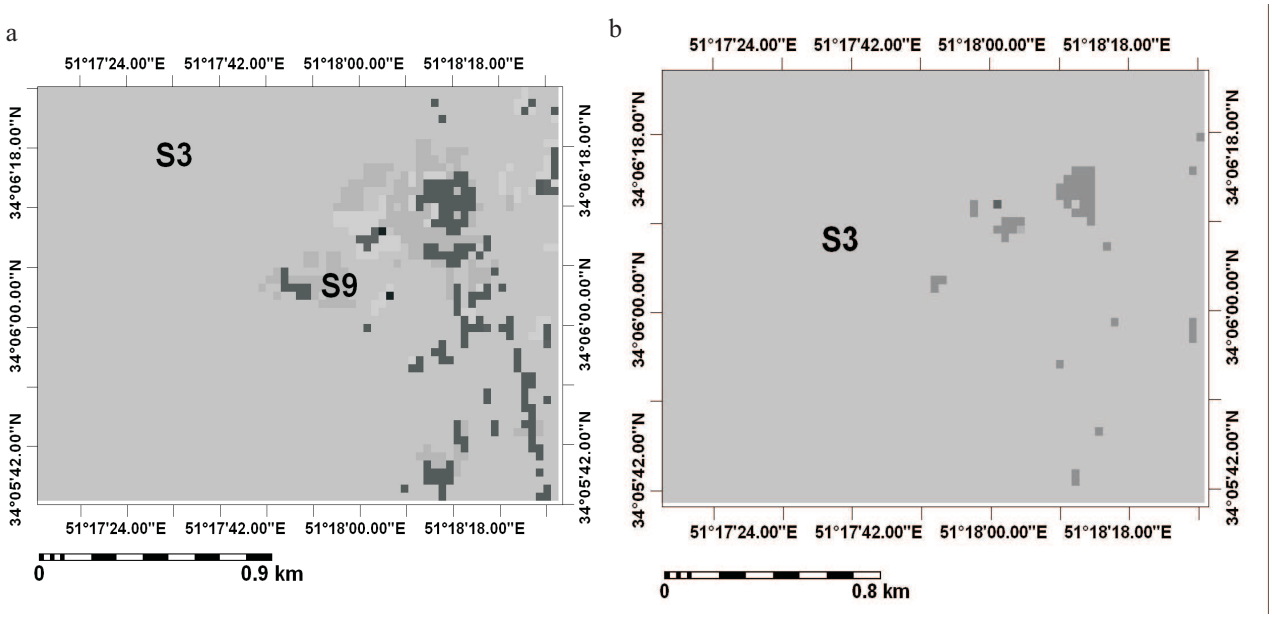

Fig. 8. Comparison separability of moist saline soils (S9) and graveled cover land (S3), a – before corporatation DEM layer in classification process, b – after DEM corporatation.

2. Soils which have soft and dark uneven surfaces are well separated in visible and thermal wave. This is because of different colour, roughness and effect of them in absorption and reflection of energy within thermal wave. But the soils are not separated in the short wave infrared bands, for the same humidity conditions of them, they have alike behaviour.

3. Land surface with gypsum and fine sand separated in all bands, especially within visible and near infrared is notable which is valuated to the surface characteristics differences.

4. The increase accuracy of classification and classes separation which have spectral interference, digital elevation model (DEM) can be added in order to separate the classes more accurately as well as increase in the overall accuracy. The comparison of band combination classification results also indicates that, use of all ASTER sensor bands, are more suitable for recognition of land use/land cover in arid and semi arid area.

REFERENCES

Aboudel-magd I. and Tantont W., 2003. Improvements in land use mapping for irrigated agriculture from satellite sensor data using a multi-stage maximum likelihood classification. Int. J. Remote Sens., 24(21), 83-95.

Ali R.R. and Kotb M.M., 2010. Use of satellite data and GIS for soil mapping and capability assessment, http://www.sciencepub.net/nature.

Breunig F.M., Galvão L.S., Formaggio A.R., and Couto E.G., 2009. The combined use of reflectance, emissivity and elevation ASTER/Tera data for tropical soil studies. R. Bras. Ci. Solo, 33, 102-107.

Buhe A., Tsuchiya K., Kaneko M., Ohtaishi N., and Halik M., 2007. Land cover of oases and forest in XinJiang, China retrieved from ASTER data. Adv. Space Res., 26, 39-45.

Chuvieco E. and Huete A., 2010. Fundamentals of Satellite Remote Sensing. CRC Press, Boca Raton, FL, USA.

Clark R.N. and Roush T.L., 1984. Reflectance spectroscopy: Quantitative analysis techniques for remote sensing applications. J. Geophys. Res., 89, 632-634.

Cloutis E.A., 1999. Agricultural crop monitoring using airborne multi-spectral imagery and c-band synthetic aperture radar. Int. J. Remote Sens., 20(4), 767-787.

Dobos E., Erika M., Marion B., Larry B., and Todd H., 2000. Use of combined digital elevation model and satellite radiometric data for regional soil mapping. Geoderma, 97, 367-391.

Fahsi A., Tsegaye T., Tadesse W., and Coleman T., 2000. Incorporation of digital elevation models with Landsat-TM data to improve land cover classication accuracy. Forest Ecol. Manag., 128, 57-64.

Jensen J.R., 1996. Introductory Digital Image Processing - a Remote Sensing Perspective.Prentice-Hall Press, London, UK.

Lillesand T.M. and Kiefer R.W., 2004. Remote Sensing and Image Interpretation. Wiley Press, New York, USA.

Law S., Law C.A.N.R., and Lishman J.R., 2003. A system for monitoring land cover. Int. J. Remote Sens., 24(23), 181-189.

Matinfar H.R., 2006. Evaluation of ASTER, LISS_III, ETM^{+}, TM and MSS data for characterizing and mapping soil base upon observation and GIS. Ph.D. Thesis,Teheran University, Iran.

Piekarczyk J., 2001. Temporal variation of the winter rape crop spectral characteristics. Int. Agrophysics, 15, 101-107.

Saito Genya N., Ishitsuka Y., and Matano K.M., 2001. Application of TERRA/ASTER data on agriculture land mapping. Proc. 22nd Asian Conf. Remote Sensing, November 5-9, Singapore.

Shalaby A. and Tateishi R., 2007. Remote sensing and GIS for mapping and monitoring land cover and land-use changes in the Northwestern coastal zone of Egypt. Appl. Geography, 27, 234-243.

Shrestha D.P. and Zinck A., 2001. Land use of image Knowledge classification in mountainous areas: integration processing, digital elevation data and field (application to Nepal). JAG, 3(1), 249-261.

Tajgardan T., Ayoubi S., Shataee S., and Sahrawat K.L., 2010. Soil surface salinity prediction using ASTER data: Comparing statistical and geostatistical models. Australian J. Basic Appl. Sci., 4(3), 303-319.

Yuan F., Sawaya K.E., Loeffelholz B.C., and Bauer M.E., 2005. Land cover classification and change analysis of the twin cities (Minnesota) metropolitan area by multitemporal LANDSAT remote sensing. Remote Sensing Environ., 98, 94-106.

Ziadat F.M., Taylor J.C., and Brewer T.R., 2003. Mergin LANDSAT TM imagery with topographic data to aid soil mapping in the Badia region of Jordan. J. Arid Environ., 54, 527-541.